Influence of thermal annealing on structural and optical properties of Au:TiO_2 nanocomposite film

A. MARIN , D. MUNTEANU*, E. ALVES[a], N.P. BARRADAS[a], L. CUNHA[b], C. MOURA[b]
Department of Materials Science and Engineering, "Transilvania" University, 500036 Brasov, Romania
[a]*Instituto Tecnológico e Nuclear, Dept. Física, Apartado 21, E.N. 10, 2686-953 Sacavém, Portugal*
[b]*Centro de Física, Universidade do Minho,4710-057 Braga, Portugal*

Two sets of nanocomposite films consisting about 4,5 at.% and 51 at.% concentrations of Au dispersed in a TiO_2 dielectric matrix were deposited by DC reactive magnetron sputtering, and subjected to several thermal annealing experiments in vacuum, for temperatures ranging from 300 to 800 ^{0}C. The thermal annealing affected the size of Au nanoparticles, and also the phase of the dielectric matrix. The obtained results show that the structure and the size of Au clusters, together with the matrix crystallinity, changed as a result of the annealing, and were shown to be able to change the optical properties of the films. The optical changes, and the correspondent Surface Plasmon Resonance effect were confirmed by reflectivity and CIELab colour measurements. X-ray diffraction (XRD) was used to determine the thin-film structure and crystallinity as a function of annealing temperature. The XRD data also shows clear evidence of the crystallization of the matrix in the anatase phase. With further increase of the annealing temperature, there is a change from anatase phase into rutile-type structure. Simultaneously, the Au atoms are organized in crystalline nanoparticles (revealing an fcc-type structure, with the (111) preferential growth orientation).

(Received May 17, 2013; accepted June 12, 2013)

Keywords: Thin films, Gold, Sputtering, Surface plasmon resonance, Magnetron Sputtering

1. Introduction

Noble metal nanoparticles thin films are an intensive area of research due to their interesting functional properties, including the possibility to have extensive colorations [1]. On the other hand, nanocomposite films consisting of noble metal nanoparticles, embedded in dielectric oxide matrixes, are being studied to be used in a wide range of applications, including those of catalysis, photocatalysis, sensors and novel optoelectronic devices [2]. One interesting feature is set when a noble metal is placed in a certain type of media, as it is the case of dielectric matrixes like that of titanium dioxide. Titanium dioxide films are extensively used in optical thin-film device applications due to their appropriate optical properties, combined with high thermal and chemical stability in hostile environments [3,4]. These films exhibit good durability, a high transmittance in the visible spectral range, and a high refractive index, and thus are suitable for applications such as antireflection coatings, multilayer optical coatings (used as optical filters), optical waveguides, and others [5]. Some investigations indicated that very thin layers of noble metals on TiO_2 surface can capture the photoinduced electrons or holes, eliminating the recombination of electron–hole pairs effectively and also extend the light response of TiO_2 in the visible light region [6,7]. Furthermore, nanoparticles of noble metals incorporated into a TiO_2 matrix are known to be able to improve its catalytic sensing and optical properties [7,8].

In the particular case of the optical properties (the driving force in the present work), their behavior depends strongly upon the nanoparticles morphology [9]. The absorption spectrum is dominated by the resonant coupling of the incident field with quanta of collective conduction electron plasma oscillations, instead of monotonically increasing with wavelength. This resonance is called Surface Plasmon Resonance (SPR), and it is dependent on the concentration, size and shape of the metal clusters and, of course, on the dielectric properties of the surrounding medium [10,11].

2. Experimental details

Two sets of Au:TiO_2 thin films (series A and B) were deposited onto silicon (100) and glass/quartz substrates by dc reactive magnetron sputtering, in a laboratory-sized deposition apparatus. For the depositions, a Ti target (99.6 % purity) was used, containing different amounts of Au pellets symmetrically incrusted in its preferential erosion zone. The number of Au pellets was varied in total amounts of 8 (series A) and 10 (series B), giving rise to two series of films with different chemical compositions. A constant dc current density of 100 Am^{-2} was applied. A mixture of argon and oxygen was injected with constant fluxes of 60 sccm and 10 sccm, corresponding to partial pressures of 0.3 Pa and 0.08 Pa, respectively. Samples were placed in a substrate holder, with a simple rotation mode (7 rpm). The substrates were biased (- 50V) and the deposition temperature was set to a value of approximately 100 °C The temperature of the coated substrates was

monitored with a thermocouple placed close to the surface of the substrate holder.

After films deposition, all samples were subjected to annealing experiments in vacuum. The annealing treatments were carried out in a vacuum furnace, after its evacuation to about 10^{-4} Pa. The selected temperature range varied from 300 to 800 °C, and the isothermal time was fixed to 60 min, after the required heating time at 5 °C/min. The chemical uniformity of the films throughout their entire thickness, for the as-deposited samples, was measured by Rutherford backscattering spectrometry (RBS), carried out in a IBA Data Furnace NDFv 9.4g at 2 MeV with ^{4}He, at an angle of incidence 0º in a small (RBS) chamber. There were three detectors in the chamber: standard at 140º, and two pin-diode detectors located symmetrical each other, both at 165º (detector 3 on same side as standard detector 2) [12].

The structure and the phase distribution of the coatings were analyzed by X-ray diffraction (XRD), using a Philips PW1710 diffractometer (Cu-Kα radiation) operating in a Bragg–Brentano configuration. XRD patterns were deconvoluted, assuming to be Voigt functions to yield the peak position and the integrated intensity. These parameters allow calculating the interplanar distance, preferential orientation and grain size. Optical properties (reflectance-transmittance) were characterized using a UV–vis-NIR Spectrophotometer (Shimadzu UV 3101 PC) in the spectral range from 250 to 800 nm. The color characterization was performed using a commercial MINOLTA CM-2600d portable spectrophotometer (wavelength range from 400 to 700 nm), using diffused illumination at a viewing angle of 8°. Color specification was computed under the standard CIE illuminant D65 (especular component excluded) and represented in the CIE 1976 L*a*b* (CIELab) color space [7,13,14].

3. Results and discussion

3.1 Composition

The Au concentration, determined by RBS analysis in the as-deposited samples was founded to be 4,5 at. % for sample A and 51,9 at. % for sample B. Table 1 summarizes some of the characteristics of the two co-deposited Au:TiO_2 samples.

Fig. 1 show the concentration profile depth, obtained by RBS, for the Au:TiO_2 as-deposited sample A and B. The elemental concentration analysis shows, that the ratio of the concentration of oxygene and titanium is always very close to the value 2, suggesting the presence of stoichiometric TiO_2 matrix. Another observation is that the gold concentration is not uniform through the film thickness. RBS analysis revealed that the gold concentration slightly varies from around 5.3 at.%, at the surface, until about 3.4 at.% close to the film/substrate interface, with an estimated average composition around 4.5 at.%. Analogous behaviour was claimed for other metal nanoparticles in thin films of similar or different matrixes, produced by other deposition techniques [15–17], and also in sol–gel Ag:TiO_2 films [18]. On the other hand, for the second set of samples (series B), the RBS analysis shows that the concentration of gold is uniform throughout the thickness and is approximately 51.9 at %, Fig.1b) .

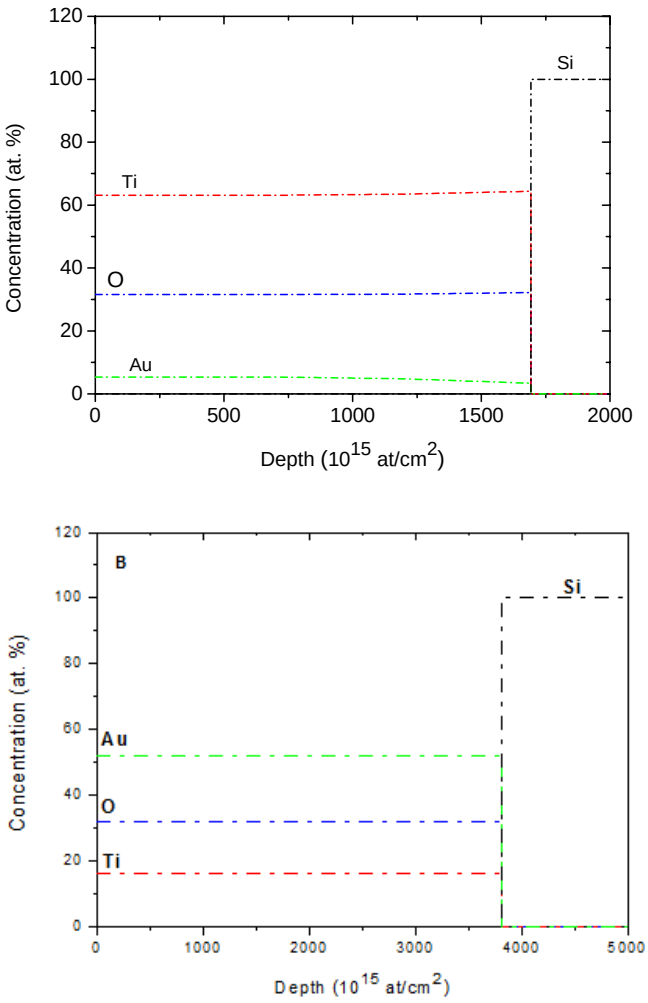

Fig. 1. Concentration profiles for sample A and B

The variation of the Au volume fraction, achieved by using theoretical approximation [19] was determined as being 0.03 for sample A and 0.37 for sample B (considering ρ(Au) = 19.30 g/cm^3 and ρ(TiO_2) = 4.23 g/cm^3). The concentration, and in consequence, the determined Au volume fraction, for each samples are very different, as expected, once the number of Au pellets that were used in each series of deposition were different. This difference, in the gold concentration of the films had influence on the optical and structural properties of the analysed samples that will be discussed in the next section.

Film series	Au pellets	Thickness (nm)	Au (at. %)	*Au volume fraction, f_{Au}
A	8	286	4.5	0.03
B	10	1037	51.9	0.37

*(Considering ρ(Au)=19.30g/cm^3 and ρ(TiO_2)=4.23g/cm^3)

3.2 Structural and Optical Characterization

The evolution of the sample's structure induced by the thermal annealing, were studied by XRD experiments. The results obtained for the both sets of samples are presented in Figure 2 and 3.

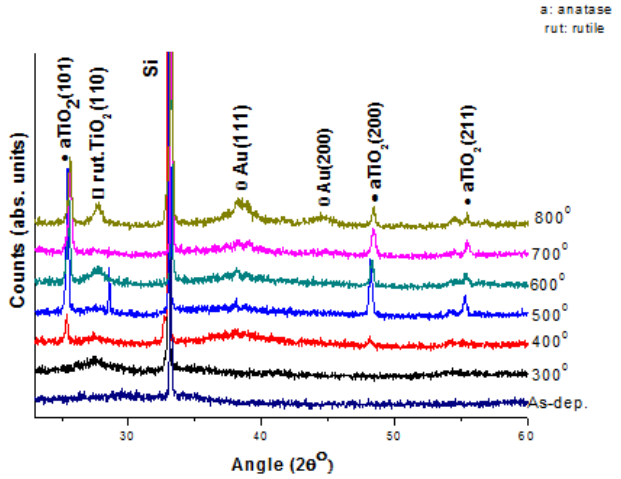

Fig. 2. XRD diffraction pattern of Au:TiO_2 sample series A as a function of the annealing temperature

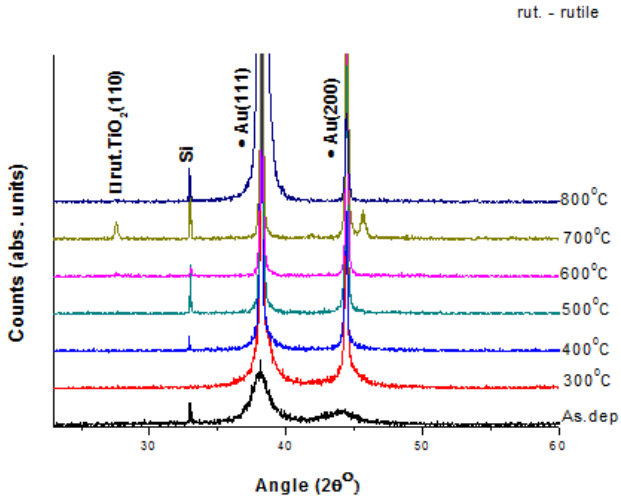

Fig. 3. XRD diffraction pattern of Au:TiO_2 sample series B as a function of the annealing temperature

For the as-deposited sample of series A, (the one with the lowest Au content) beside the features of (100) silicon substrates, no diffraction peaks were obtained from any known crystalline phase of the binary Ti–O compounds or traces of crystalline Au. The crystallization of the amorphous films starts to be detected at the annealing temperature of 300 ºC, by the identification of signatures related with the TiO_2 matrix, particularly from the rutile and anatase phases. The presence of Au, in sample A, starts to be evidenced for annealing temperatures above 400^{0}C, as it can be observed by the emergence of the (111) peak, localized at 2θ= 38,26^o. The detection of the Au (200) peak, at 2θ = 44,60^0 only occurs at the annealing temperature of 800ºC. These results show that the expected formation of Au clusters, was partally achieved. In fact, the formation of these clusters, is evidenced, in the XRD patterns, by the presence of Au peaks which become narrower with increasing temperature [9]. It was also reported [16] that the observation of SPR activity was achieved for Au composition ranges between 10 – 20 at. %. In this set of samples (A) the Au volume fraction is very low (0.03) and the estimated average composition was around 4.5 at.%. As it will be discussed later, the reflectivity analysis, will confirm that this set of samples didn't fulffil the conditions to obtain an SPR activity. Regarding the second set of samples (B), produced with higher Au content, the XRD patterns, displayed in figure 3, already reveal the presence of Au difraction peaks in the as-deposited sample. Two peaks are detected, centered at 2θ = 38.2° and 2θ = 44.4°. These peaks should be assigned, respectively, to the (111) and (200) planes of the Au fcc structure. These peaks become narrower and more intense with the increase of the annealing temperature. This behaviour is due to the formation of Au nanoclusters in the TiO_2 matrix. In these samples the first trace of crystallization of theTiO_2 matrix only appears at annealing temperatures above 600ºC, and only the signature of rutile TiO_2 phase is detected.

The average diameter of the gold particles in the nanocomposite films, were determined from the integral breadth analysis and Scherrer equation of the XRD Au peaks. For the samples A, only for the sample annealing at 800ºC was possible to determine the grain size, since, as it was already point out the detection of the Au (200) peak only occurs at this temperature, and the average diameter was 4.8 nm. For the samples with higher content in gold, the results, of the average diameter, are shown in in Figure 4. This figure clearly illustrates a continuous increasing on the Au particles (clusters) that ranges from about 5 nm for the as-deposited sample to approximately 77.3 nm for the sample annealed at 700^{0}C, followed by a decrease in the grain size for the annealed sample at 800ºC. The decrease in the grain size observed for this sample could be related with diffusion of gold on the sample, enhanced by the relatively high temperature. The SPR activity and the related changes on the optical properties are directly affected by this growth.

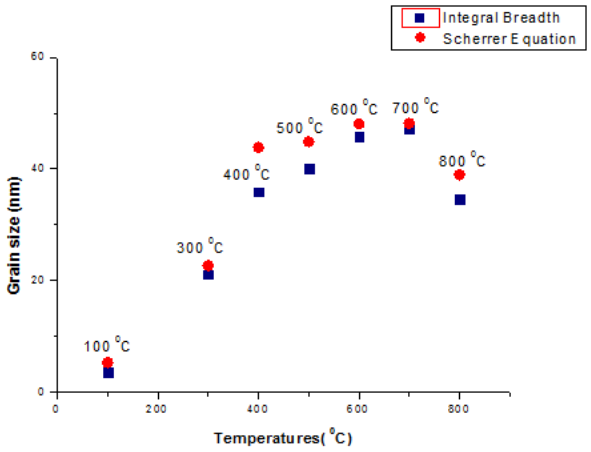

Fig. 4 Variation of grain size of Au crystallites as a function of annealing temperature

For the as-deposited sample of series A, (the one with the lowest Au content), the visual inspection of its surface revealed a green-blue tone, characteristic of an interference-like behavior, that has changed with the annealing experiments to a red-brownish tone. These variation on the color of samples were quantified in CIE $L^*a^*b^*$ color space that is illustrated in Figure 5. For samples A the yellowness (b^*) and the lightness (L^*) decrease where the color contribution from red/green goes in the positive a^* direction.

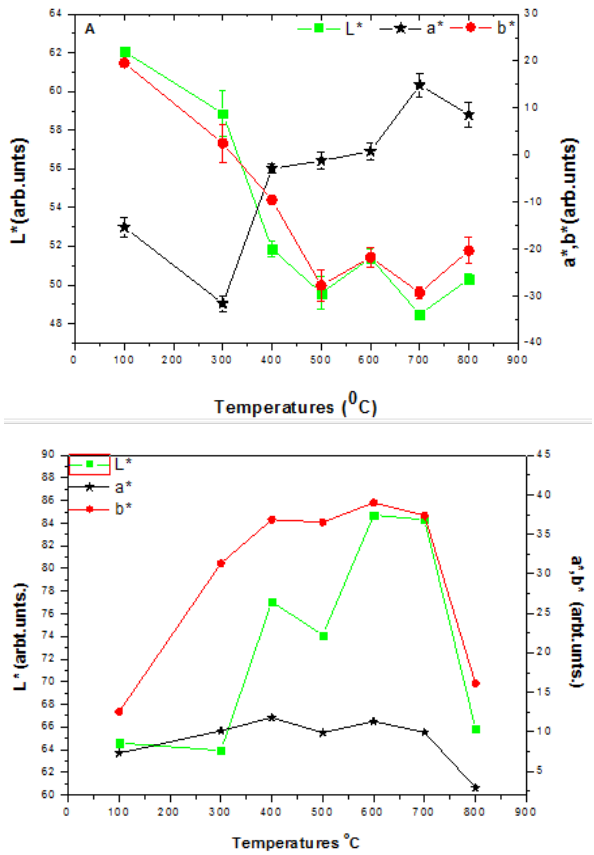

Fig. 5. The color variation of samples A (a) and samples B (b) quantified by $L^*a^*b^*$ as function of annealing temperature

The interferometric optical behaviour of the sample of A series is clearly seen in the reflectivity spectra displayed in Fig. 5 a). In this figure are shown only the results of the as-deposited and of the annealed sample at 400^0C and 700^0C, to be able to clearly visualize the results. In this series, the intrinsic golden-like color was never reached, even for the highest annealing temperatures. As, it was pointed out, these samples presented an Au concentration below 5 at.%, that is already in the lower limit of concentration to have an intrinsic response for this kind of nanocomposites[14].

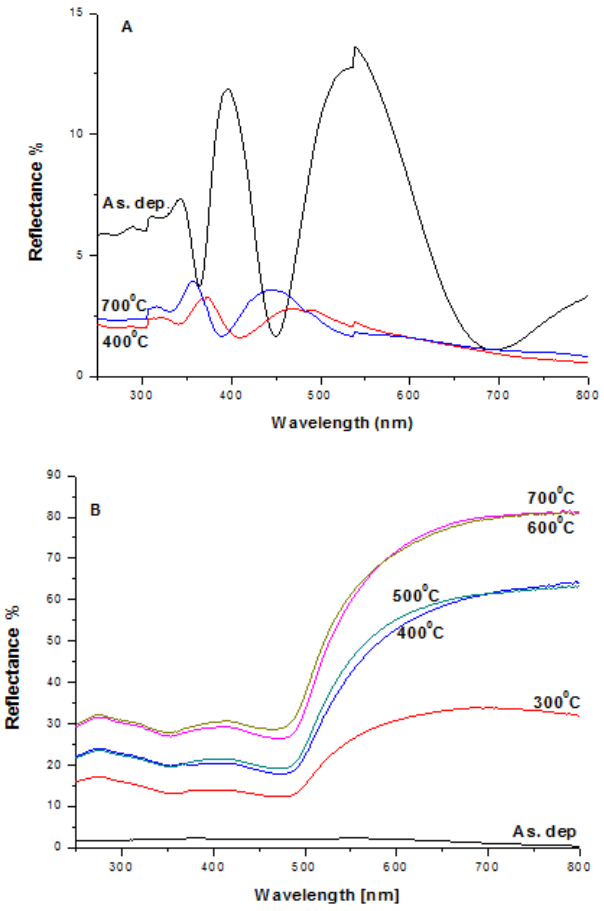

Fig. 6. Variation of reflectivity as a function of annealing temperature (a) for series A, (b) for series B.

Different reflectivity behavior was found for the samples from series B, characterized by a higher quantity of gold embedded in the TiO_2 matrix.. From the variation on the color of these set of samples shown in Fig. 5 b) it is possible to see that these samples become more yellow and redder, the a^* and b^* parameter increases with the annealing temperature, with a slight increase on the darknes. The reflectivity spectra, displayed in figure 6 b), shows that no interferometric behaviour is seen. The spectra also shows that the reflectivity profiles are typical from samples with an intrinsic colour, that in this case was a golden metallic one. For the as-deposited sample the reflectivity value is lower than 5% and it is almost constant, for the entire wavelength range. As the annealing

temperature increases there is an expected increase in the reflectivity of the samples, particularly for the highest wavelengths in the visible region of the electromagnetic spectra. The samples annealed at temperatures up to 700 ^oC reveal that the locations of the reflectivity curve minima are slightly shifting to lower wavelengths (473 nm at 300 ^oC to 462 nm for 700 ^oC).

Moreover, the optical behavior of the post-annealed series B is actually very similar to that obtained for "pure" gold. The higher reflectivity of the "pure" gold sample is due to its bulk morphology. As reported for "pure" TiO_2 the reflectivity of the as-deposited film does not show any unexpected optical behavior [20].

4. Conclusions

The deposited films were subjected to annealing treatments at different temperatures.

The structural conditions are influenced by two different parameters, amount of Au gold doping the dielectric TiO_2 matrix and grain size of the Au nanoclusters that can be controlled by the annealing temperatures of the samples after the deposition.

Reflectivity on the visible spectrum range and CIELab color values show a direct relation with the annealing temperature which is changing the grain size of gold clusters embedded in the dielectric matrix**.**

All the changes on the optical properties are consistent with the changes on crystal grain size studied on the XRD profiles.

To conclude, we have shown that the "one step" co-sputtering of a Ti-Au target, followed by an appropriate thermal treatment, is a useful way to produce composite TiO_2/Au films with adjustable nanostructure and, consequently, controllable SPR-related optical properties and color.

Acknowledgments

This paper is supported by the Sectoral Operational Programme Human Resources Development (SOP HRD), ID76945 financed from the European Social Fund and by the Romanian Government.

This work was supported by FEDER through the COMPETE Program and by the Portuguese Foundation for Science and Technology (FCT) in the framework of the Strategic Project PEST-C/FIS/UI607/2011.

References

[1] G. Walters, I .P.P arkin, J. Mater .Chem. **19**, 574 (2009)

[2] M. G. Manera, J. Spadavecchia, D. Busoc, C. de Julian Fernandez, G. Mattei, A. Martucci, Mulvaney, J. Perez -Juste, R. Rella, L. Va sanelli, P. Ma zzoldi, Sens. Act. B **132**, 107 (2008)

[3] B. Karunagaran, R.T. Rajendra Kumar, D. Mangalaraj, S.K. Narayandass, G. Mohan Rao, Cryst. Res.Technol. **37**, 1285 (2002)–1292.

[4] D. Mardare, P. Hones, Mater. Sci. Eng. B **68**, 42 (1999).

[5] R.C. Adochitea, D. Munteanu, M. Torrell, L. Cunha, E. Alves, N.P. Barradas, A. Cavaleiro, J.P. Riviere, E. Le Bourhis, D. Eyidi, F. Vaz, The influence of annealing treatments on the properties of Ag:TiO_2 nanocomposite films prepared by magnetron sputtering, Appl. Surf. Sci. (2012)

[6] H. Y. Chuang, D. H. Chen, Nanotechnology **20**(105), 70 4 (2009)

[7] R. C. Adochite , M. Torrell, L. Cunha, E. Alves, N. P. Barradas A. Cavaleiro, J. P. Riviere, D. Eyidii, F. Vaz, Optoelectron. Adv. Mater. – Rapid Commun **5**(1), 73 (2011).

[8] N. P . Barradas, C. Jeynes ,R.P. Webb , Appl. Ph ys. Lett. **71** , 291 (1997)

[9] M. Torrell, R. Kabir, L. Cunha, M. Vasilevskiy, F. Vaz, A. Cavaleiro, E. Alves, Journal of applied physics 109,(2011).

[10] E. Hutter, Janos H. Fendler, Adv. Mater. **16**, 1685 (2004).

[11] V. Shutthanandan, Y. Zhang, S. Thevuthasan, L.E. Thomas, W.J. Weber, G. Duscher, C.M. Wang, Nucl. Instrum. Methods Phys. Res. Sect. B **242**, 448 (2006).

[12] N. P. Barradas, C. Jeynes, M.A. Harry, Nucl. Instr. and Meth. B **136**, 1163 (1998).

[13] H. Ehrenreich, H. R. Philipp, Phys. Rev. **128**, 1622 (1962).

[14] M. Torrell, P. Machado, L. Cunha, N. M. Figueiredo, J. C. Oliveira, C. Louro, F. Vaz, Surf. Coat. Technol. **204**, 1569 (2010).

[15] C. Sella, S. Chenot, V. Reillon, S. Berthier, Thin Solid Films **517**, 5848 (2009).

[16] L. Armelao, D. Barreca, G. Bottaro, A. Gasparotto, C. Maccato, E. Tondello, O. Lebedev, S. Turner, G. Van Tendeloo, C. Sada, U. Lavrencic Stangar, Chem. Phys. Chem. **10**, 3249 (2009).

[17] A. Gibaud, S. Hazra, C. Sella, P. Laffez, A. Desert, A. Naudon, G. Van Tendeloo, Phys. Rev. B **63**, 193407 (2001).

[18] J. Won Yoon, T. Sasaki, N. Koshizaki, J. Sol-Gel Sci. Technol. **22**, 115 (2001).

[19] Juan Wang, W.M. Lau, Quan Li, J. App. Phys. **97**(11), 114303 (2005).

[20] Hiroshi Yoshida, Hiroyuki Nasu, Kanichi Kamiya, Jun Matsuoka, J. Sol-Gel Sci. Technol. **9**(2), 145 (1997).

*Corresponding author: muntean.d@unitbv.ro